



University of Dundee

Probabilistic prediction of cavitation on rotor blades of tidal stream turbines

Chernin, Leon; Val, Dimitri V.

Published in:
Renewable Energy

DOI:
[10.1016/j.renene.2017.06.037](https://doi.org/10.1016/j.renene.2017.06.037)

Publication date:
2017

Document Version
Peer reviewed version

[Link to publication in Discovery Research Portal](#)

Citation for published version (APA):

Chernin, L., & Val, D. V. (2017). Probabilistic prediction of cavitation on rotor blades of tidal stream turbines. *Renewable Energy*, 113, 688-696. <https://doi.org/10.1016/j.renene.2017.06.037>

General rights

Copyright and moral rights for the publications made accessible in Discovery Research Portal are retained by the authors and/or other copyright owners and it is a condition of accessing publications that users recognise and abide by the legal requirements associated with these rights.

- Users may download and print one copy of any publication from Discovery Research Portal for the purpose of private study or research.
- You may not further distribute the material or use it for any profit-making activity or commercial gain.
- You may freely distribute the URL identifying the publication in the public portal.

Take down policy

If you believe that this document breaches copyright please contact us providing details, and we will remove access to the work immediately and investigate your claim.

Probabilistic prediction of cavitation on rotor blades of tidal stream turbines

Leon Chernin^a and Dimitri V. Val^{b,*}

^a *School of Engineering, Physics and Mathematics, University of Dundee, Dundee DDI 4HN, United Kingdom*

^b *Institute for Infrastructure & Environment, Heriot-Watt University, Edinburgh EH14 4AS, United Kingdom*

Abstract

Power generation from tidal currents is currently a fast developing sector of the renewable energy industry. A number of technologies are under development within this sector, of which the most popular one is based on the use of horizontal axis turbines with propeller-type blades. When such a turbine is operating, the interaction of its rotating blades with seawater induces pressure fluctuations on the blade surface which may cause cavitation. Depending on its extent and severity, cavitation may damage the blades through erosion of their surface, while underwater noise caused by cavitation may be harmful to marine life. Hence, it is important to prevent cavitation or at least limit its harmful effects. The paper presents a method for predicting the probability of cavitation on blades of a horizontal axis tidal stream turbine. Uncertainties associated with the velocities of seawater and water depth above the turbine blades are taken into account. It is shown how using the probabilistic analysis the expected time of exposure of the blade surfaces to cavitation can be estimated.

Keywords: Tidal stream turbine, rotor blades, cavitation, turbulence, waves, probability

Highlights:

- A probabilistic approach to predicting the cavitation on the rotor blades of a tidal stream turbine is proposed
- Probabilistic models describing uncertainties associated with the velocities of seawater and water depth above the turbine blades are introduced
- A case study illustrating the application of the new probabilistic approach as well as an existing deterministic approach is presented
- It is shown that the existing deterministic approach does not provide sufficient data for rational and economically efficient design of tidal stream turbines for cavitation

* Corresponding author: Tel.: +44 1314514622; fax: +44 1314514617.
E-mail address: d.val@hw.ac.uk

1. Introduction

Harnessing the kinetic energy of tidal currents is a fast developing sector of the renewable energy industry [1, 2]. A horizontal axis turbine with propeller-type blades is one of the popular devices used for this purpose. During the turbine operation its rotating blades interact with flowing seawater. This interaction causes pressure fluctuations on the blade surfaces and may lead to the inception of cavitation. Cavitation is a process of formation of gas-vapour structures in a liquid when pressure reduces below a certain critical level at constant ambient temperature [3, 4]. The possibility of cavitation inception on the turbine blades is supported by experimental evidence [2, 5-8] and computational studies [9-11]. Depending on the blade geometry, hydrodynamic conditions and fluid properties, a number of cavitation forms can develop on the turbine blades: blade tip vortex cavitation, leading edge sheet cavitation and back side bubble cavitation [4, 6, 7, 9]. Numerical modelling of cavitation inception on the turbine blades indicated that cavitation clouds could cover up to two thirds of the blade [9]. Experimental investigation showed that the sheet cavitation could extend over 20% of the blade chord from its leading edge becoming unstable at the sheet tail end and transforming into the cloud cavitation [6]. Cavitation, depending on its extent and severity, can cause breakdown of turbine operation, blade surface erosion, noise and vibration [6, 7]. In particular, cavitation erosion can damage the turbine blades by removing the protective coating and exposing the blade shell to aggressive marine environment, followed by gradual damage to the blade shell material. The latter weakens the blades and negatively affects the turbine performance so that eventually the blade replacement is required. The possibility of cavitation inception can be reduced by limiting the rotational speed of the turbine rotor, shortening the blades and placing the rotor deeper under water. However, these measures negatively affect the power production efficiency of such a turbine [12]. Thus, cavitation is one of the major factors influencing the design of a tidal stream turbine and the choice of its operational conditions [2]. The need in maximising the power production drives the engineers towards the limits in ‘cavitation-safe’ design. So far, the evaluation of cavitation inception on the turbine blades has been carried out using a deterministic approach, aimed at keeping the blades out of the ‘cavitation window’ (i.e. completely avoiding the cavitation inception) (e.g., [8, 10, 11]). However, there are significant uncertainties associated with seawater velocities and quality, the distance from the sea surface to the turbine blades and a model used to estimate the pressure distribution on the blade surface. Under such

conditions the use of probabilistic analysis, which explicitly takes into account the uncertainties, is advantageous.

Both deterministic and probabilistic approaches are used in this paper for the evaluation of cavitation inception on the rotor blades of a pitch-controlled tidal stream turbine. The main purpose of this evaluation and based on it design is to prevent (or limit) damage to the turbine blades due to cavitation erosion. In this context, the most damaging form of cavitation is cloud cavitation, which can develop from sheet and bubble cavitation [4]. Thus, although the inception of tip vortex cavitation may occur earlier than that of sheet cavitation the former is not considered in the paper. To simplify further analysis the engineering definition of cavitation is adopted, according to which cavitation occurs at a certain point on the blade surface when the local pressure at this point drops below the vapour pressure of seawater [4]. The distribution of the pressure (or the pressure coefficient, C_p , representing it) around the blade surface is derived using the 2D vortex panel code XFOIL [13]. The deterministic approach is used to evaluate the minimum depth of the turbine rotor for given turbine and tidal current parameters to avoid cavitation inception. In principle, cavitation may cause damage to the blade surface in a relatively short period of time since the time history of a small transient bubble is measured in milliseconds [3]; however, a noticeable damage does not occur instantaneously but accumulates over time. By that reason, the probabilistic approach is employed to estimate the expected time of exposure of the blade surfaces to cavitation. In accordance to the adopted definition of cavitation, the blade surface is assumed to be exposed to cavitation whenever the local pressure is below the seawater vapour pressure. The model used in the probabilistic approach takes into account uncertainties associated with the velocities of seawater and water depth above the turbine blades. Uncertainties associated with the temperature and salinity of seawater, as well as the model for calculation of C_p are not considered in the analysis due to insufficient data for their quantification; however, they can easily be taken into account if such data are available. An important parameter affecting cavitation, which is also not considered in the following analysis, is the water quality (i.e. nuclei content) [4]. In this case, in addition to the lack of data to quantify uncertainties associated with this parameter and its influence on cavitation, taking it into account would significantly increase the complexity of the cavitation prediction. Thus, in order to keep the analyses, in particular probabilistic analysis, reasonably simple this phenomenon is omitted from consideration in this study.

2. Modelling cavitation inception

It is assumed that cavitation occurs at a point on the blade surface where the local pressure, P_L , drops below the vapour pressure of seawater, P_V (e.g., [4, 8])

$$P_L \leq P_V \quad (1)$$

The local pressure consists of the contributions of the pressure applied by the flowing seawater, P_F , the atmospheric pressure, P_{AT} , and the immediate hydrostatic pressure of seawater, ρgH

$$P_L = P_F + P_{AT} + \rho gH \leq P_V \quad (2)$$

where H is the immediate distance from the seawater surface to the point under consideration on the blade surface, g the acceleration of gravity ($= 9.81 \text{ m/s}^2$) and ρ the density of seawater ($= 1025 \text{ kg/m}^3$). Rearranging Eq. (2) and dividing its both sides by $0.5\rho U_{tot}^2$ leads to

$$-\frac{P_F}{0.5\rho U_{tot}^2} \geq \frac{P_{AT} + \rho gH - P_V}{0.5\rho U_{tot}^2} \quad (3)$$

or

$$-C_p \geq Ca \quad (4)$$

where $C_p = P_F/(0.5\rho U_{tot}^2)$ is the pressure coefficient, $Ca = (P_{AT} + \rho gH - P_V)/(0.5\rho U_{tot}^2)$ the cavitation number and U_{tot} the total velocity of the flow around the considered section along the blade. U_{tot} is defined as a combination of the flow velocity through the rotor disk, $U(z,t)(1-a)$, and the tangential velocity of the blade section, $\omega r(1+a_\omega)$ (see Figure 1)

$$U_{tot} = \sqrt{[U(z,t)(1-a)]^2 + [\omega r(1+a_\omega)]^2} \quad (5)$$

where $U(z,t)$ is the upstream velocity of seawater at the distance z from the seabed at time t , a and a_ω the axial and tangential induction factors, respectively, ω the angular velocity of the rotor and r the distance along the blade from the rotor axis to the considered blade section (e.g., at the blade tip r equals the rotor radius R).

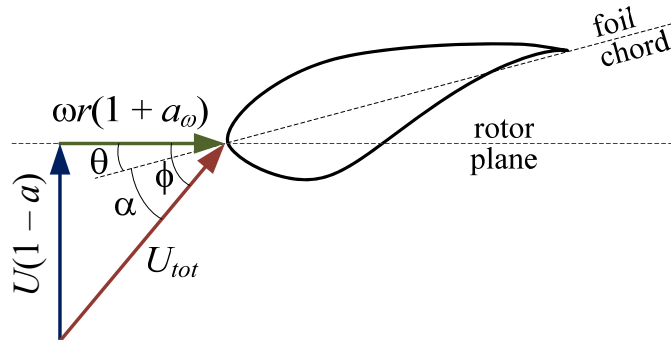


Figure 1. Total flow velocity at the rotor plane

The distribution of pressure applied by seawater on the blade surface depends on the angle of attack, α , which is the angle between the plane of the blade foil chord and the direction of U_{tot} (see Figure 1) and can be expressed as

$$\alpha = \phi - \theta \quad (6)$$

where θ is the angle between the rotor plane and the chord of the foil and ϕ is the angle between the rotor plane and the direction of U_{tot} . In pitch-controlled turbines θ equals the sum of the immediate pitch angle of the blade, θ_p , and the local twist angle of the considered blade section, θ_t

$$\theta = \theta_p + \theta_t \quad (7)$$

whereas ϕ can be found as (see Figure 1)

$$\phi = \tan^{-1} \frac{U(z,t)(1-a)}{\omega r(1+a_\omega)} \quad (8)$$

Two approaches are applied to the analysis of cavitation inception on the surface of rotor blades of a tidal stream turbine, namely, (i) deterministic and (ii) probabilistic. In the deterministic approach, the minimum distance from the sea surface to the rotating blade required to prevent cavitation inception is determined using the model described above. All parameters appearing in the model are treated as constants or deterministic functions. The latter concerns $U(z,t)$, which is represented by the average current velocity, $\bar{U}(z,t)$. For simplicity, the variation of the average current velocity over time, $\bar{U}(t)$, takes into consideration only the main semi-diurnal cycle with the period $T_1 = 12.4$ hours and the spring-neap-spring cycle with the period $T_2 = 14.8$ days (or 354.4 hours) so that

$$\bar{U}(t) = \left[K_0 + K_1 \cos\left(\frac{2\pi t}{T_1}\right) \right] \cos\left(\frac{2\pi t}{T_2}\right) \quad (9)$$

where the coefficients K_0 and K_1 depend on the maximum average velocities in spring and neap tides. The variation of $\bar{U}(z,t)$ over the water depth, i.e., tidal current profile, is described by the 1/7th power law [14]

$$\begin{aligned} \bar{U}(z,t) &= \left(\frac{z}{0.32h} \right)^{1/7} \bar{U}(t) & 0 \leq z \leq 0.5h \\ \bar{U}(z,t) &= 1.07\bar{U}(t) & 0.5h < z \leq h \end{aligned} \quad (10)$$

where h is the total water depth.

In the probabilistic approach, the probability of cavitation, i.e., the probability that C_p exceeds Ca , and based on that the expected time of cavitation over a given time period are estimated. Uncertainties associated with the velocity of seawater and the water depth above the blade surface are taken into account. In this case, $U(z,t)$ is expressed as the sum of the average tidal current velocity, $\bar{U}(z,t)$, and the fluctuations, $u(z,t)$, caused by turbulence, $u_t(t)$, and wind waves, $u_w(z,t)$, i.e.,

$$\begin{aligned} U(z,t) &= \bar{U}(z,t) + u(z,t) \\ u(z,t) &= u_t(t) + u_w(z,t) \end{aligned} \quad (11)$$

To simplify the analysis, the spatial variability of turbulence is not considered and only the horizontal particle velocity due to wind waves is taken into account.

To account for uncertainty of the water depth, the distance H in Eq. (3) is presented as

$$H = h_{im} + h_{tw} + h_{ww} \quad (12)$$

where h_{im} is the immediate depth of the considered blade section for the mean sea level, which varies cyclically due to the rotation of the turbine rotor, h_{tw} the depth change induced by a tidal wave and h_{ww} the surface elevation due to a wind wave. According to Eq. (3), the possibility of cavitation inception is the highest near the blade tip when the blade passes through the top region of the turbine rotor disk. This occurs because compared to other blade sections the blade tip has the highest tangential velocity and at the top point its distance to the water surface is minimal so that Ca has the smallest values. Further in the paper only cavitation on this section of the blade is considered. To apply the probabilistic approach models describing the turbulence, tidal wave, wind waves and their interaction with tidal current are needed and will be described in the following sections.

It is important to note that the implementation of this cavitation inception model is based on the blade element momentum theory and the 2D vortex panel code XFOIL [13]. As a result, the model can only account for the leading edge sheet cavitation and front/back side bubble cavitation developing on the blade segment near the blade tip, while the vortex cavitation which may occur right at the blade tip is ignored. This simplification seems reasonable since the sheet and bubble cavitation can become unstable and develop into the cloud cavitation, which is among the most damaging cavitation types [4, 6].

3. Turbulence model

Turbulence is characterised by its intensity, I_u , which is defined as the ratio of the standard deviation of the velocity fluctuations caused by turbulence, σ_u , to the average velocity, i.e.,

$$I_u = \frac{\sigma_u}{U} \quad (13)$$

According to available data, I_u depends on the average current velocity and for current velocities faster than 1.5 m/s is about 10%, e.g., [15]. Another characteristic of turbulence required in various turbulence models is the integral length scale, L . There are limited data about this characteristic. It has been suggested that for an open channel L can be set approximately equal to 0.8 of the channel depth [16]. Stochastic properties of turbulence are described by its power spectrum (or spectral density), $S_u(f)$, which is obtained by the Fourier transform of the autocorrelation of $u_{tr}(t)$, where f represents the frequency of fluctuations. In this paper the tidal flow turbulence is described by the von Karman spectrum, which in non-dimensional form can be expressed by as

$$\frac{f S_u(f)}{\sigma_u^2} = \frac{4 f L / \bar{U}}{[1 + 70.78 (f L / \bar{U})^2]^{5/6}} \quad (14)$$

It is also assumed that $u_{tr}(t)$ is a stationary Gaussian process with zero mean and standard deviation σ_u .

4. Modelling of waves

4.1 Tidal wave

Assuming that the tidal wave amplitudes are small compared to the water depth and the depth is relatively small compared to the wavelength, the tidal wave can be modelled as a purely progressive wave [17]. This formulation adopts a linear relationship between the height of the tidal wave and the velocity of the tidal current. The changes of the depth introduced by the tidal wave can then be calculated as

$$h_{tw} = \bar{U}(t)(d/g)^{1/2} \quad (15)$$

where d is the depth of water at the location of the turbine corresponds to the mean sea level. This is obviously a simplistic approach since Eq. (15) does not take into account possible effects of shoaling/funnelling, damping due to bottom friction, reflection against the estuary

boundaries and deformation due to differences in velocities of flood and ebb tides. $\bar{U}(t)$ can take both positive (flood tide) and negative (ebb tide) values. The latter are of higher importance for cavitation inception since they correspond to the reduction of the height of the water column and, consequently, of Ca .

4.2 Wind waves

Only short-term variations of wind waves are considered. According to [18], the random variable representing the wave height, H_w , is then can be modelled by the following Rayleigh distribution

$$F_{H_w}(h_w) = 1 - \exp\left[-\left(\frac{h_w}{\alpha_H H_s}\right)^2\right] \quad (16)$$

where H_s is the significant wave height and $\alpha_H = 0.5\sqrt{1-\rho}$. The parameter ρ represents band width effects of the wave spectrum and typically is in the range -0.75 to -0.6. The distribution of the wave period, T_w , is conditional on the wave height

$$F_{T_w|H_w}(t_w|h_w) = \Phi\left(\frac{t_w - \mu_{T_w}}{\sigma_{T_w|H_w}}\right) \quad (17)$$

where $\Phi(\cdot)$ is the standard normal cumulative distribution function and

$$\begin{aligned} \mu_{T_w} &= C_1 T_{w1} \\ \sigma_{T_w|H_w} &= C_2 \frac{H_s}{h_w} T_{w1} \end{aligned} \quad (18)$$

The coefficients C_1 and C_2 depend on the mean wave period T_{w1} .

4.3 Wave-current interaction

The above wave model is applicable in the absence of current. However, tidal current is present in the problem considered herein. Hence, the interaction between the waves and the current should be considered since it affects both the wave height and the particle velocity associated with the wave. In the following, a reasonably simple approach for taking into account the wave-current interaction is described. It is assumed that the waves are linear and the current is slow varying (i.e., it changes little over a wave length) and uniform. The latter contradicts the current velocity variation over depth previously introduced by Eq. (10). However, it was found in the past that linear waves over a current flow of nearly 1/7th power form responded only to the surface current velocity [19]. Thus, for the purpose of modelling

the wave-current interaction, the current velocity, U_c , will be taken equal to $1.07\bar{U}$. It is also assumed that the current and wave directions are parallel, i.e., the current is either following or opposing the waves, and the current is negligible outside the region of the turbine location. These are reasonable assumptions when the turbine is located in a narrow strait.

The dispersion relation in this case is (e.g., [20])

$$\omega_w = \sqrt{gk_c \tanh(k_c d)} + k_c U_c \quad (19)$$

where $\omega_w = 2\pi/T_w$ is the apparent (or absolute) angular wave frequency and k_c the wave number in the presence of tidal current. This wave number is unknown but can be found by numerically solving Eq. (19). It should be noted that when the current is opposing the waves Eq. (19) may not have a solution for k_c or yield a negative number. This means that the waves are blocked by the current at the strait entrance.

After k_c has been calculated, the wave height in the region with the tidal current (i.e., within the strait), H_{wc} , can be found based on the conservation of wave action as [20]

$$H_{wc} = H_w \sqrt{\frac{C_g}{C_{gc} + U_c} \frac{\omega_{wc}}{\omega_w}} \quad (20)$$

where ω_{wc} is the intrinsic (or relative) angular wave frequency, C_g and C_{gc} the wave group velocities without and with tidal current, respectively. These parameters can be calculated using the following formulae:

$$\omega_{wc} = \sqrt{gk_c \tanh(k_c d)} \quad (21)$$

$$C_g = \frac{\omega_w}{2k} \left[1 + \frac{2kd}{\sinh(2kd)} \right] \quad (22)$$

$$C_{gc} = \frac{\omega_{wc}}{2k_c} \left[1 + \frac{2k_c d}{\sinh(2k_c d)} \right] \quad (23)$$

where k is the wave number in the region without tidal current, which can be found by either solving Eq. (19) with $U_c=0$ or using an approximate formula given in [18]. In addition, it has been shown that in the case of opposing current waves usually oversteepen and break before the actual blocking condition is reached [21]. To check if this happens H_{wc} needs to be compared with the breaking wave height, $H_{w,max}$, which can be estimated using Miche's criterion [25]

$$H_{w,max} = \frac{0.28\pi}{k_c} \tanh(k_c d) \quad (24)$$

i.e., $H_{wc} > H_{w,max}$ means that the waves break near the strait entrance.

If the waves are blocked or break then u_w in Eq. (11) and h_{ww} in Eq. (12) are equal to zero. Otherwise, they are calculated as

$$u_w(z, t) = \frac{H_{wc} \omega_{wc}}{2} \frac{\cosh(k_c z)}{\sinh(k_c d)} \cos(\omega_{wc} t) \quad (25)$$

$$h_{ww} = \frac{H_{wc}}{2} \cos(\omega_{wc} t) \quad (26)$$

where $z = d - h_{im}$.

5. Case study

5.1 Turbine design and location

The phenomenon of cavitation is studied in this paper on the example of a horizontal axis pitch-controlled turbine with a three-bladed rotor. The selection of the turbine parameters is explained in detail in [22]. The turbine is intended to produce 1 MW power before losses at the rated current velocity of 2.6 m/s, its operating current velocity range is 1 – 3.5 m/s. The rotor diameter is 18 m (i.e., its radius $R = 9$ m). The turbine has a fixed rotational speed $\omega = 14$ rpm and its power coefficient is slightly above 0.45 [22]. The turbine blades are designed using NREL S814 foil [23]. The blade geometry is such that the twist of the blade tip is 4° . The pitch angle of the turbine blades changes when the average current velocity, \bar{U} , exceeds its rated value to ensure the production of the rated power. Table 1 shows the relationship between \bar{U} and the pitch angle obtained from the analysis of the turbine performance.

Table 1: Pitch angle vs. \bar{U}

\bar{U} (m/s)	Pitch, θ_p ($^\circ$)
1.0	0.0
2.6	0.0
2.7	4.4
2.8	6.0
2.9	7.3
3	8.4
3.1	9.4
3.2	10.3
3.3	11.2
3.4	12.1
3.5	12.9

It has been recommended to select the rotor diameter as 50% of the water depth at the turbine location and place the rotor hub at the midpoint of the depth [24]. In accordance to

these recommendations, it is assumed that the turbine is located in 36 m deep waters and its hub is 18 m from the seabed. It has also been assumed that the significant wave height at the turbine location is 4 m and the mean wave period is 8 s, i.e., $H_s = 4$ m and $T_{w1}=8$ s, and that $\rho = -0.7$. For such wave conditions values of the coefficients C_1 and C_2 in Eq. (18) can be selected as 1.20 and 0.22, respectively [18]. It is also assumed that at the turbine location the maximum values of \bar{U} in spring and neap tides are 3.5 m/s and 1.7 m/s, respectively. The corresponding values of the coefficients K_0 and K_1 in Eq. (9) are 2.6 m/s and 0.9 m/s, respectively.

5.2 Induction factors

In order to find the angle of attack α and U_{tot} , values of the axial and tangential induction factors (a and a_ω) need to be known (see Figure 1). These values have been calculated for the tip segment of the blade using the NWTC Subroutine Library [25], which is based on the blade element momentum theory. It has been found that a and a_ω depend on both $\bar{U}(z,t)$ and u (see Eq. (11)). However, for simplicity the dependency of a_ω on u has been neglected since it has been checked that the influence of a_ω on U_{tot} is less than 1%. The following relationships between a and $\bar{U}(z,t)$ and u , and a_ω and $\bar{U}(z,t)$ have been obtained by regression analysis:

$$a = |a_0 + a_1 u + a_2 u^2| \quad (27)$$

$$a_0 = \begin{cases} -0.0573\bar{U}(z,t) + 0.5317 & \bar{U}(t) \leq 2.6 \text{ m/s} \\ -1.4876\bar{U}(z,t) + 4.5107 & 2.6 < \bar{U}(t) \leq 2.7 \text{ m/s} \\ 71.8468\bar{U}^{-5.4862}(z,t) & \bar{U}(t) > 2.7 \text{ m/s} \end{cases} \quad (28)$$

$$a_1 = \begin{cases} -0.0077\bar{U}(z,t) - 0.0395 & \bar{U}(t) \leq 2.6 \text{ m/s} \\ 1.6023\bar{U}(z,t) - 3.0161 & 2.6 < \bar{U}(t) \leq 2.7 \text{ m/s} \\ -0.04911\bar{U}^2(z,t) + 0.3274\bar{U}(z,t) - 0.4820 & \bar{U}(t) > 2.7 \text{ m/s} \end{cases} \quad (29)$$

$$a_2 = \begin{cases} -0.0033\bar{U}(z,t) + 0.0013 & \bar{U}(t) \leq 2.6 \text{ m/s} \\ -0.1373\bar{U}(z,t) + 0.3741 & 2.6 < \bar{U}(t) \leq 2.7 \text{ m/s} \\ 0.0151\bar{U}(z,t) - 0.0660 & \bar{U}(t) > 2.7 \text{ m/s} \end{cases} \quad (30)$$

$$a_\omega = \begin{cases} 0.0025\bar{U}(z,t) - 0.0017 & \bar{U}(t) \leq 2.6 \text{ m/s} \\ -0.0127\bar{U}(z,t) + 0.0407 & 2.6 < \bar{U}(t) \leq 2.7 \text{ m/s} \\ -0.0033\bar{U}(z,t) + 0.0133 & \bar{U}(t) > 2.7 \text{ m/s} \end{cases} \quad (31)$$

5.3 Minimum pressure coefficient

The pressure coefficient is expressed as

$$C_p = \frac{P_F}{0.5\rho U_{tot}^2} \quad (32)$$

The distribution of P_F (and so of C_p) over the blade surface depends on the angle of attack α , which defines the direction of U_{tot} in relation to the blade foil chord and is influenced by changes in the values of \bar{U} and u . According to the cavitation inception model given in Eq. (4), the cavitation occurs initially at the point on the blade surface where the pressure coefficient is at its minimum value, i.e., $-C_{p,min}$. Therefore, Eq. (4) can be written as

$$-C_{p,min} = Ca \quad (33)$$

The value and location of $C_{p,min}$ on the blade surface can be found from the distribution of C_p over the blade tip segment and can be connected to α through a $-C_{p,min}$ vs. α diagram. This diagram can be seen as a type of the cavitation bucket diagram (e.g., see [8]) and is derived in this study for the NREL S814 foil and the range of values of α between -25° and 25° . The 2D vortex panel code XFOIL [13] was found in the past to be suitable for the calculation of C_p [8] and used in this study to obtain values and locations of a $C_{p,min}$. XFOIL utilises a linear-vorticity second order accurate panel method coupled with an integral boundary-layer method and an e^n -type transition amplification formulation. The Newton solution procedure is used in this software for computing of the inviscid/viscous coupling. The NREL S814 foil has been modelled in XFOIL using 280 panels. The panels varied in length and were distributed by the default XFOIL's panelling routine non-uniformly around the foil perimeter.

The adopted range of α ($-25^\circ \div 25^\circ$) is deemed to cover all possible combinations of the following angles: twist $\theta_r = 4^\circ$, pitch θ_p corresponding to the turbine operating range of \bar{U} (see Table 1) and the angles generated by the seawater velocity fluctuations due to turbulence and wind waves $u = \pm 0 \div 5$ m/s. The resulting $-C_{p,min}$ vs. α diagram is shown in Figure 2, where each point represents one simulation. The analysis of the C_p distributions derived for the considered range of α indicates that $C_{p,min}$ occurs at three different points on the foil surface shown in Figure 3. The $-C_{p,min}$ vs. α diagram can be divided into four regions where one of these points is dominant (see Figure 2). Figure 4 depicts examples of distributions of C_p on the foil surface for each region, i.e., $\alpha = -15^\circ$ for Region 1 where Point 3 is dominant, $\alpha = -5^\circ$ for Region 2 where Point 1 is dominant, $\alpha = 2^\circ$ for Region 3 where Point 2 is dominant

and (d) $\alpha = 9^\circ$ for Region 4 where Point 3 is dominant. Note that Figure 4 presents C_p curves obtained using viscous (solid curves) and inviscid (dashed curves) flow, while only the viscous flow simulation results were used in this study. From the analysis of Figure 4 follows that these three points (shown in Figure 3) define zones with lowest C_p on the foil surface. The abscissae of the three points along the foil chord are as follows:

- Point 1: $-C_{p,min}$ occurs at the front side at $x = 0.2182$
- Point 2: $-C_{p,min}$ occurs at the back side at $x = 0.2944$
- Point 3: $-C_{p,min}$ occurs at the foil leading edge

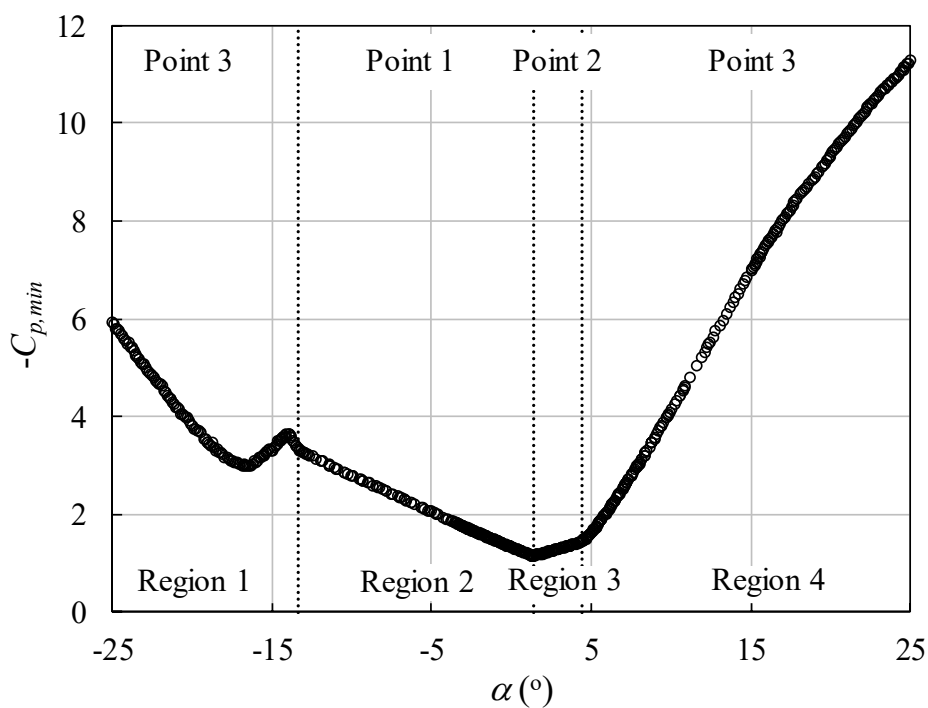


Figure 2. $-C_{p,min}$ vs. α diagram

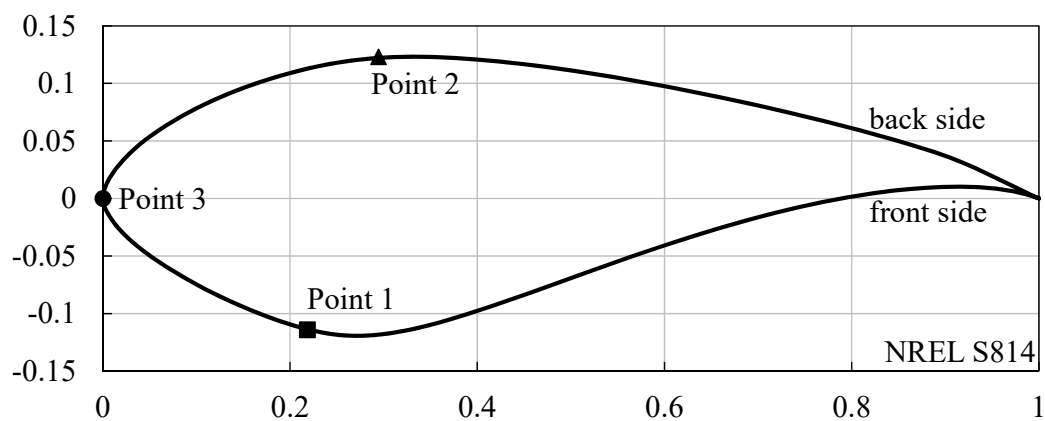


Figure 3. Locations of $-C_{p,min}$ on NREL S814 foil.

It is important to note that experiments carried out on small scale turbine prototypes [6, 7] showed that sheet cavitation developed at the leading edge and extended over a part of the back (suction) side of the blade at its top half. Additionally, bubble cavitation developed on the back side of the blade away from the leading edge. Figures 3, 4a and 4b additionally suggest that in pitch controlled tidal stream turbines, cavitation (possibly bubble cavitation) can also occur on the front (pressure) side of the blade for very low and negative values of the angle of attack.

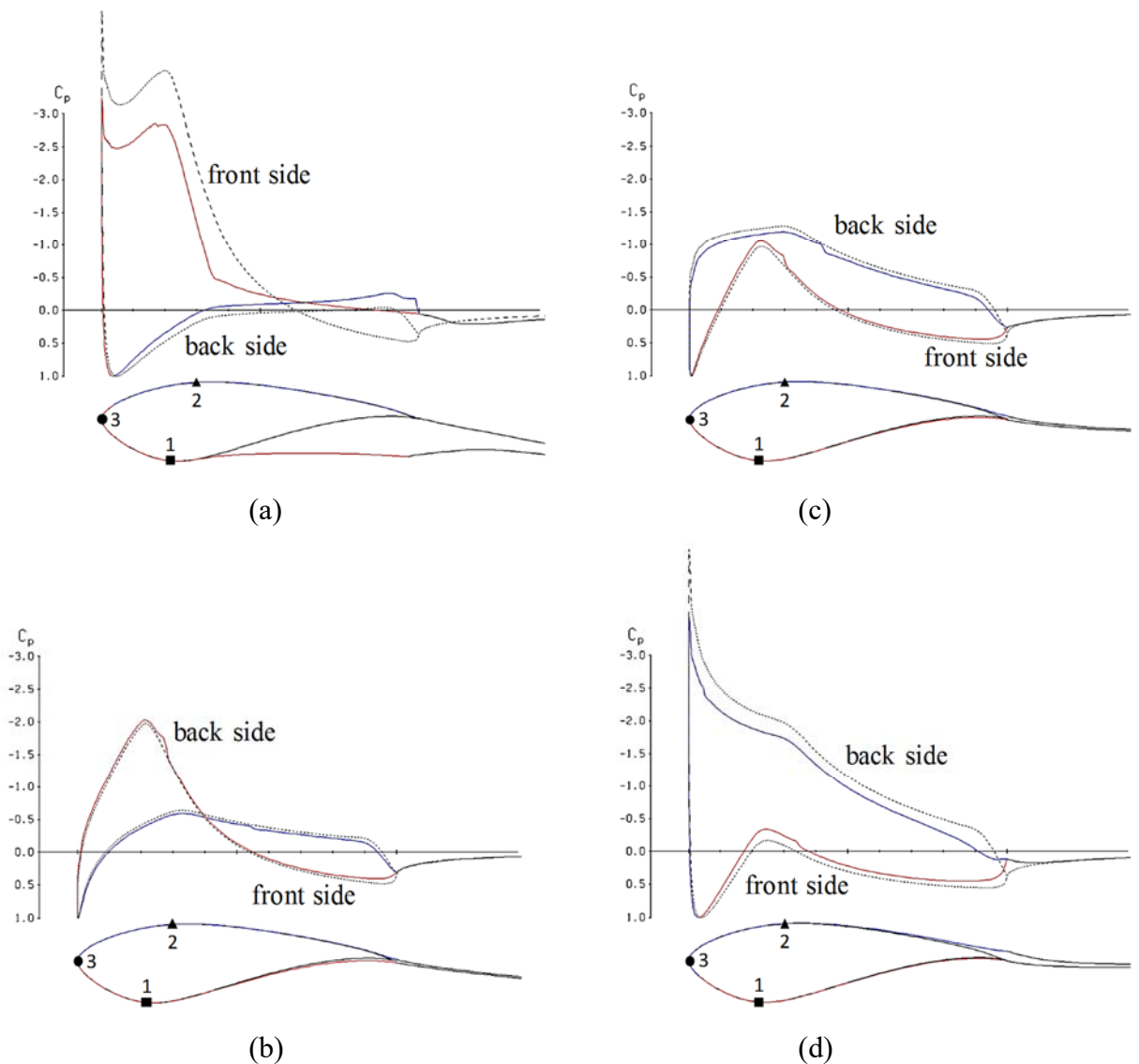


Figure 4. Distributions of C_p on back and front sides of NREL S814 foil for (a) $\alpha = -15^\circ$, (b) $\alpha = -5^\circ$, (c) $\alpha = 2^\circ$ and (d) $\alpha = 9^\circ$. The dashed curves represent inviscid flow while solid curves viscous flow. The figure also shows flow separation at the foil trailing edge.

5.4 Deterministic analysis

The aim of the deterministic analysis is to find the minimum water depth to the tip of the rotating blade that is required to prevent cavitation, i.e., to ensure that $-C_{p,min} < Ca$. It starts with derivation of the $-C_{p,min}$ vs. \bar{U} relationship. This relationship (rather than the $-C_{p,min}$ vs. α diagram in Figure 2) is used here for its convenience, since only \bar{U} varies while the velocity fluctuations u are ignored and the angular velocity of the rotor is constant. Figure 5 shows that the $-C_{p,min}$ vs. \bar{U} curve is piecewise with three distinct maximum points corresponding to the minimum (1 m/s), rated (2.6 m/s) and maximum (3.5 m/s) operating current velocities. Additionally, $-C_{p,min}$ occurs at different places on the blade surface with increasing \bar{U} , i.e., it occurs on the front side of the blade (at Point 1) for relatively low and high \bar{U} and on the back side (at Point 2) for intermediate \bar{U} close to the rated velocity. The locations of Points 1 and 2 on the surface of the blade tip segment are shown in Figure 3. The relationship between Ca and \bar{U} has then been calculated for various values of H (see Eq. (3)) until the condition $-C_{p,min} \geq Ca$ has been reached for $H = 5.3$ m at \bar{U} just below 3.5 m/s (see Figure 5). This means that if the distance from the sea surface to the rotor blades is greater than 5.3 m then according to the deterministic approach there should be no cavitation inception on the blade surface within the operating current velocity range.

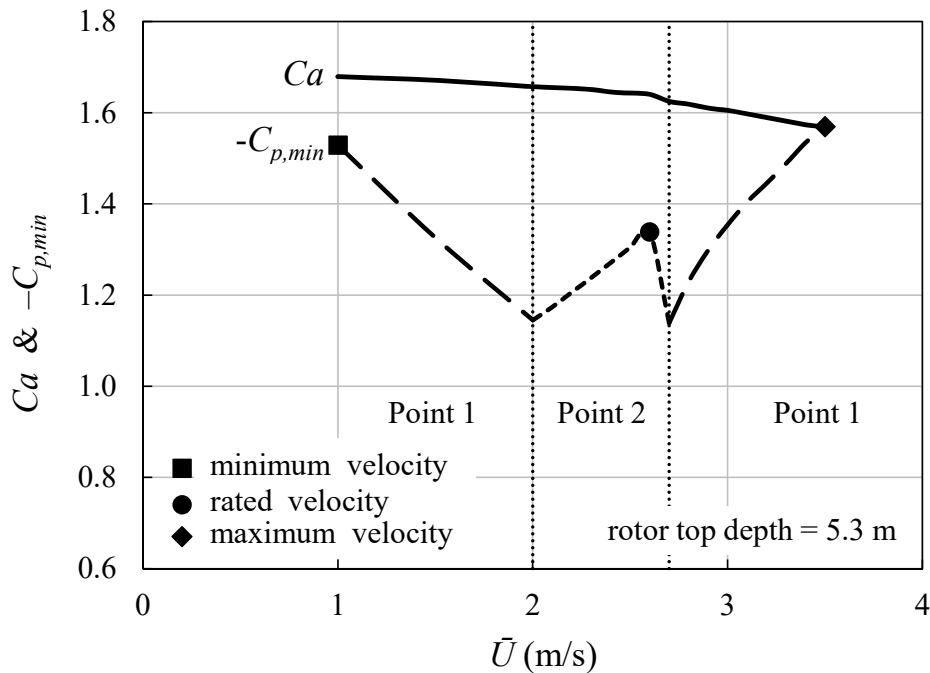


Figure 5. Ca and $-C_{p,min}$ vs. \bar{U} for $H=5.3$ m.

5.5 Probabilistic analysis

The probabilistic approach is aimed to estimate the expected time of the blade surface exposure to cavitation during a given time interval (e.g., the design life of the rotor blades). To achieve that the probability of cavitation (i.e. of $-C_{p,min} \geq Ca$) is initially estimated for different possible values of \bar{U} . This is carried out using Monte Carlo simulation. For a given value of \bar{U} (e.g., -2.6 m/s) 100,000 samples are generated. Each sample represents the time of passage of one wind wave over the turbine. Thus, for each sample the wind wave height is first generated in accordance to Eq. (16) followed by the generation of the wave period in accordance to Eq. (17). The wave period is then converted to the relative wave period $T_{wc} = 2\pi/\omega_{wc}$ to take into account the wave-current interaction; if a wave is blocked or breaks the duration of the sample is set equal to 10 s. In each sample, the initial position of the considered blade is also randomly generated. The time interval associated with each sample is divided into 0.2 s subintervals. For each subinterval, a value of the stochastic process representing rapid fluctuations of the current velocity due to turbulence $u_{tr}(t)$ is generated in accordance to the previously described model using the inverse Fourier transform (for more detail see [22]). The variation of the wind wave height over the turbine and the change of the blade position due to rotation are considered so that values of h_{im} and h_w are changing from one subinterval to another as well as values of $u_w(z,t)$ and $\bar{U}(z,t)$ (for the latter this occurs due to its variation over the water column in accordance to Eq. (10)). The expected relative time of cavitation exposure for a given value of \bar{U} is then the ratio of the number of subintervals within which cavitation inception occurs to the total number of the subintervals in 100,000 samples. It is worth to note that almost the same procedure can be used to estimate the distribution of the relative time of cavitation exposure if more information about this random variable than just its expected value is needed. In this case, instead of directly aggregating results for all 100,000 samples the ratios are calculated separately for each sample and then, based on these results, a histogram of the relative time of cavitation exposure is constructed.

Results of the analysis are shown in Figure 6. As can be seen, the highest probability of cavitation is during ebb tides at the highest operating current velocity of -3.5 m/s. It drops sharply at lower average velocities and then increases again at the rated current velocity of -2.6 m/s. For the ebb current velocity below -1.6 m/s the probability of cavitation is less than 1×10^{-3} . The probability of cavitation is low for flood tides; the highest value is 1.3×10^{-3} for the rated current velocity of 2.6 m/s.

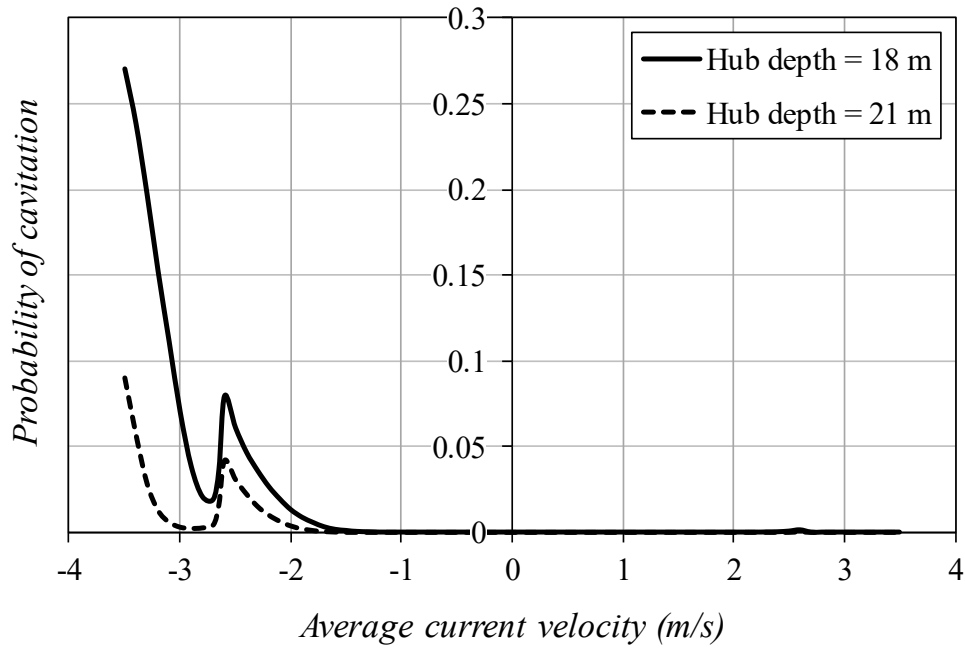


Figure 6. Probability of cavitation vs. \bar{U} .

To estimate the expected time of cavitation exposure for a given time interval the results presented in Figure 6 are combined with Eq. (9) so that the function of the probability of cavitation vs. lifetime of the turbine during the spring-neap-spring cycle is obtained – see Figure 7. Numerically integrating this function over the duration of the cycle and then dividing the result by this duration yields the expected relative time of cavitation exposure. For the considered example it equals 0.014. This means that for, e.g., 10-year service life the surface of the blade near its tip will be exposed to cavitation on average 51 days.

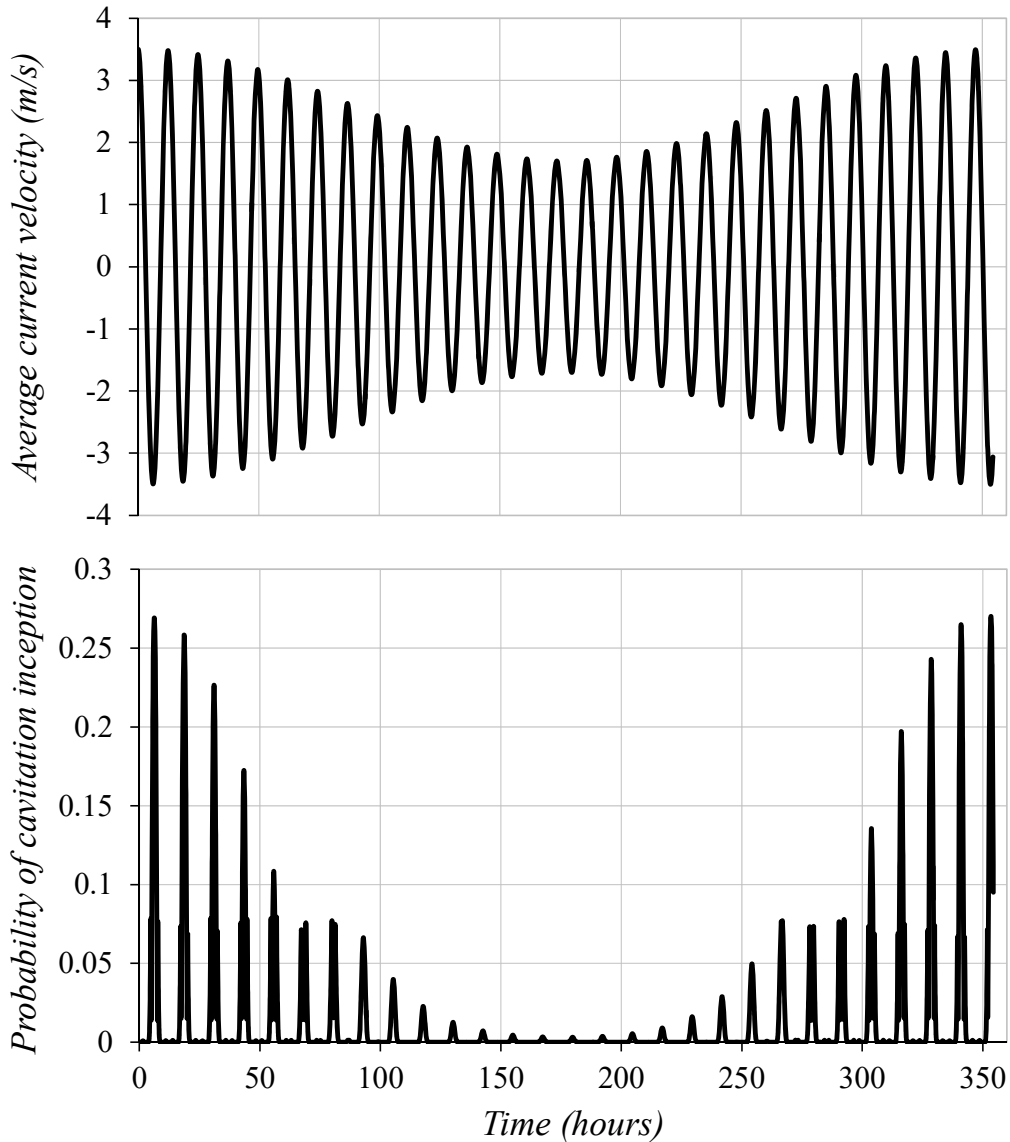


Figure 7. Probability of cavitation exposure over the spring-neap-spring cycle.

Next, let's compare the deterministic and probabilistic approaches. According to the deterministic approach the water depth of 5.3 m above the rotor blades is needed to prevent cavitation inception. If to take into account the maximum change of the depth due to an ebb tidal wave at $\bar{U} = -3.5$ m/s, which is 6.7 m, this means that the turbine rotor hub should be 21 m below the mean sea level, i.e., placed 3 m deeper underwater. This will decrease the turbine efficiency in terms of power production and increase its cost but not completely eliminate the possibility of cavitation. The probability of cavitation vs. \bar{U} has been also calculated for this case and the results are shown in Figure 6. As can be seen, the probability of cavitation has decreased but is it acceptable now or should the turbine be placed even deeper underwater? In order to answer this question a model predicting the accumulation of

damage caused by cavitation to the blade material over time is needed. The model should relate the level of damage induced by cavitation with the time that the blade has been exposed to it. In addition, an acceptable level of the damage (e.g. cavitation erosion remains within the incubation period), i.e. limit state, and the corresponding target probability of failure need to be defined. The latter can be determined from economic considerations. The design of turbine blades for cavitation is then should ensure that the probability of failure (i.e. probability of violating the limit state) does not exceed its target value. The probability of failure can be calculated by using the model for cavitation-induced damage to construct a curve relating the probability of exceeding the specified level of damage with a given time of cavitation exposure and then combining this curve with the distribution of the relative time of cavitation exposure obtained by the procedure presented in this paper. Uncertainties associated with a cavitation-induced damage model can be naturally taken into account in such an analysis. Thus, the probabilistic approach can answer the above question and provide a rational and efficient tool for the design of tidal turbine blades for cavitation. However, there is currently no model capable to predict cavitation-induced damage (i.e. erosion) in composite materials of tidal turbine blades so that further experimental and numerical studies are needed before the probabilistic approach can be implemented in design practice.

Returning to the deterministic approach, it is incapable by itself to answer what values of uncertain parameters (e.g. water depth, velocity of seawater) should be used in the design for cavitation to ensure that the turbine blades do not suffer unacceptable damage but, at the same time, the turbine power production is not unnecessarily negatively affected. For example, if the static head (i.e. water depth) above the blades is to be determined by taking into account the wave height what value of the latter should be used (e.g. mean, mean plus standard deviation, etc.)? Similar, what value should be added to the seawater velocity to account for the fluctuations due to turbulence? By taking larger and larger values of these parameters, the probability of cavitation will be further and further reduced but the design will become more overconservative and inefficient. The problem can be resolved by initially employing the probabilistic approach to determine what values of the uncertain parameters (or corresponding safety factors) should be used in the design to ensure that the probability of failure (i.e. of unacceptable cavitation-induced damage) does not exceed its target value. This would then exclude the need for carrying out a complex probabilistic analysis each time when the blades of a tidal turbine are designed for cavitation and in essence similar to the calibration of modern design standards (e.g. [26]). Since in such an approach the values used

in deterministic design have been derived based on probabilistic analysis it would more correct to refer to the approach as semi-probabilistic rather than deterministic.

In the probabilistic analysis various sources of uncertainty, e.g., uncertainties associated with the seawater properties (i.e. temperature, salinity) and quality (i.e. nuclei content) and the employed models, have been neglected. Taking them into account will lead to an increase of the probability of cavitation and, subsequently, of the expected time of cavitation exposure. Eq. (15) does not account for a number of important factors affecting tidal waves and, as a result, usually overestimates the height of such waves. At the same time, the value of the significant wave height ($H_s = 4$) used for modelling wind waves may either increase or decrease depending on the turbine location. Thus, among the factors not fully considered in this analysis there are the ones that lead to an increase of the time of cavitation exposure and those that lead to a decrease of this time. Their effects need to be further investigated in the future.

It is also worth to note that the blade design used in the paper could probably be improved in terms of cavitation avoidance, e.g. by pitch reduction near the blade tip or increase in the blade chord. However, it would not completely eliminate the probability of cavitation. Thus, the above analyses and discussion would still be valid although the $-C_{p,min}$ vs. α diagram (Figure 2) would change.

6. Conclusions

A probabilistic approach to the evaluation of cavitation on blades of tidal stream turbines has been presented. Although not all major sources of uncertainty associated with such analysis have been taken into account it has been demonstrated that the blades of a tidal turbine may be exposed to cavitation over relatively long periods of time during their service life even when a deterministic analysis predicts that cavitation inception is not possible. Moreover, it has been explained that the current deterministic approach does not provide sufficient information for rational design of tidal turbine blades for cavitation. For such design, an approach based on the combination of probabilistic estimation of the expected time of cavitation exposure and a model for prediction of cavitation-induced damage in the blade material can be very beneficial. However, in order to implement this approach models of material damage by cavitation are needed.

References

- [1] King J, Tryfonas T. Tidal stream power technology – state of the art. In: Proceedings of Oceans'09 IEEE. Bremen, Germany; 2009.
- [2] Fraenkel PL. Power from marine turbines. Proceedings of the Institution of Mechanical Engineers, Part A: Journal of Power and Energy, 2002; 216, 1-14.
- [3] Knapp RT, Daily JW, Hammit F. Cavitation. McGraw-Hill; 1970.
- [4] Kim KH, Chahine G, Franc JP, Karimi A. Advanced experimental and numerical techniques for cavitation erosion prediction. Springer; 2014.
- [5] Bahaj AS, Myers LE. Cavitation prediction in operating marine current turbines. Renewable energies in maritime island climates. In: Proceedings of Conference C67 of the Solar Energy Society, Belfast, Northern Ireland; 2001.
- [6] Wang D, Atlar M, Sampson R. An experimental investigation on cavitation, noise, and slipstream characteristics of ocean stream turbines. Proceedings of the Institution of Mechanical Engineers, Part A: Journal of Power and Energy, 2006; 221(2), 219-231.
- [7] Bahaj AS, Molland AF, Chaplin JR, Batten WMJ. Power and thrust measurements of marine current turbines under various hydrodynamic flow conditions in a cavitation tunnel and a towing tank. Renewable Energy, 2007; 32(3), 407-426.
- [8] Molland AF, Bahaj AS, Chaplin JR, Batten WMJ. Measurements and predictions of forces, pressures and cavitation on 2-D sections suitable for marine current turbines. Proc. of the Institution of Mechanical Engineers, Part M: Journal of Engineering for the Maritime Environment 2004; 218, 127-38.
- [9] Guo Q, Zhou LJ, Wang ZW. Numerical simulation of cavitation for a horizontal axis marine current turbine. In: Proceedings of International Symposium of Cavitation and Multiphase Flow (ISCM 2014), IOP Conference Series: Materials Science and Engineering, 72; 2015.
- [10] Barber RB, Motley MR. A numerical study of the effect of passive control on cavitation for marine hydrokinetic turbines. In: Proceedings of 11th European Wave and Tidal Energy Conference Series, EWTEC2015, Nantes, France; 2015.
- [11] Gracie K, Nevalainen TM, Johnstone CM, Murray RE, Doman DA, Pegg MJ. Development of a blade design methodology for overspeed power-regulated tidal turbines. In: Proceedings of 11th European Wave and Tidal Energy Conference Series, EWTEC2015, Nantes, France; 2015.

- [12] Fraenkel P. Practical tidal turbine design considerations: a review of technical alternatives and key design decisions leading to the development of the SeaGen 1.2MW tidal turbine. In: Proceedings of Ocean Power Fluid Machinery Seminar, Institution of Mechanical Engineers, London; 2010.
- [13] Drela M. XFOIL: An analysis and design system for low Reynolds number airfoils. In: Proceedings of the Conference on Low Reynolds Number Aerodynamics. University of Notre Dame, Indiana; 1989.
- [14] HSE. Environmental considerations. Offshore Technology Report 2001/010, Health & Safety Executive, Norwich; 2002.
- [15] Thompson J, Polagye B, Richmond M, and Durgesh V. Quantifying turbulence for tidal power applications. In: Proceedings of Oceans'10 MTS/IEEE, paper 100514-042. Seattle, USA; 2010.
- [16] Nezu I, Nakagawa H. Turbulence in Open-Channel Flows. Balkema; 1993.
- [17] Pugh DT. Tides, surges, and mean sea level. John Wiley & Sons; 1987.
- [18] DNV. Environmental conditions and environmental loads. DNV-RP_C205. Det Norske Veritas; 2007.
- [19] Thomas GP. Wave-current interactions: an experimental and numerical study. Part 1. Linear waves. Journal of Fluid Mechanics, 1981; 110, 457-474.
- [20] Smith JM. One-dimensional wave-current interaction. CETN IV-9. U.S. Army Engineer Waterways Experimental Station, Coastal Engineering Research Center; 1997.
- [21] Chawla A, Kirby JT. Monochromatic and random wave breaking at blocking points. Journal of Geophysical Research, 2002; 107(C7), 3067.
- [22] Val DV, Chernin L, Yurchenko DV. Reliability analysis of rotor blades of tidal stream turbines. Reliability Engineering & System Safety, 2014; 121, 20-33.
- [23] Somers DM. The S814 and S815 Airfoils. Airfoils, Inc., State College, PA; 1992.
- [24] Bryden IG, Naik S, Fraenkel P, Bullen CR. Matching tidal current plants to local flow conditions. Energy, 1998; 23(9), 699–709.
- [25] Buhl ML. NWTC Design Codes (NWTC Subroutine Library); 2004. [Online]: http://wind.nrel.gov/designcodes/miscellaneous/nwtc_subs/
- [26] EN 1990:2002 Eurocode: Basis of structural design. CEN 2005.